Theory of pseudoelasticity and the shape-memory effect

Y. Yamada
Institute for Solid State Physics, The University of Tokyo, Roppongi, Minato-ku, Tokyo 106, Japan
(Received 25 February 1992)

A theory of pseudoelasticity has been developed in the phenomenological Ginzburg-Landau scheme. The system characterized by "stripe"-type ferroelastic domain structure has been discussed using the transfer-integral method, which directly gives the equilibrium density of domain boundaries and the response of domain pattern against the external stress. The results are applied to the case of a $Pb_3(PO_4)_2$ crystal, an ionic material that exhibits pseudoelasticity and shape-memory effect. It is suggested that in this particular case, the built-in random stress field is mainly responsible for pseudoelastic behavior. The observed stress-strain curve has been analyzed from this standpoint. The origin of the observed two-way shape-memory effect has been also inferred qualitatively from the same standpoint.

I. INTRODUCTION

The shape-memory effect and pseudoelasticity have been known as the remarkable elastic properties exhibited by several bcc-based alloys which undergo a martenistic phase transformation. The physical origin of these remarkable properties are at least conceptually well understood as follows.[1] The bulk deformation under stress is caused by the displacement of the twin boundaries between variants of martensite, not by introduction of lattice defects. The pseudoelasticity is expected if the motion of the domain boundaries is reversible. Even if the domains are pinned by some extrinsic defect, the twins are annihilated on heating through the transition, which results in the recovery of the original bulk shape.

As for theoretical treatment of these phenomena, there are attempts to discuss the stress-strain curve within the framework of a Landau-type thermodynamical treatment.[2–4] However, since a Landau-type treatment deals with a spatially uniform system, the mechanism of pseudoelasticity which includes the motion of twin boundaries is certainly beyond the scope of this type of theory. So far, quantitative theoretical approaches to describe pseudoelastic responses of bulk crystals have been lacking.

The purpose of this paper is to develop a thermodynamical theory of pseudoelasticity based on the Ginzburg-Landau scheme. In the GL scheme, the order parameter is allowed to be spatially varying, and the domain boundary is expressed by a kink-type solution of the r-dependent order parameter. This suggests the possibility to develop a thermodynamics of domain structure in which the quantities such as equilibrium distribution of kinks (domain boundaries), the response of kinks against the external force, the interkink interaction, etc., should be the central issues.

In principle, any ferroelastic material has the possibility to exhibit the same elastic properties because the necessary condition is the existence of variants of spontaneous strains. In fact, ionic crystals $LnNbO_4$ (Ln: La, Nd) were reported to show remarkable pseudoelasticity.[5,6] Recently, it was reported that $Pb_3(PO_4)_2$ also exhibits pseudoelasticity and two-way shape memory at room temperature.[7] It was confirmed that the pseudoelasticity of this material is caused by the reversible motion of the ferroelastic domain boundaries just as in the case of alloys. Another interesting aspect of $Pb_3(PO_4)_2$ was recently found in connection with the structural characteristic above the transition temperature:[8] the observed x-ray diffraction spectrum at $T > T_c$ shows a peculiar precursor phenomena called the "ghost lattice" effect.[9–11] It is noticeable that the same precursor phenomena have been also observed in various shape-memory alloys.[12,13] These facts suggest that the elastic properties of $Pb_3(PO_4)_2$ have definite similarity to those of shape memory alloys.

On the other hand, to carry out a detailed theoretical analysis, $Pb_3(PO_4)_2$ has the advantage that the phase transition mechanism of this material has been well established within a Landau-type phenomenological scheme.[14,15] The order parameters are specified unambiguously, and the free energy is explicitly expressed in terms of the order parameters. This information will provide the basis to discuss the thermoelastic properties of this material.

We therefore discuss here the particular case of $Pb_3(PO_4)_2$, in order to take advantage of the fact that the Landau-type treatment has been established in this material, so that the extension to GL scheme is straightforward. However, considering the close similarity of the phenomena observed in this material to other SM materials we expect this investigation to provide a model treatment for pseudoelasticity and the shape memory effect in general.

II. REVIEW OF EXPERIMENTAL RESULTS

In this section we briefly review the experimental results on pseudoelasticity and shape-memory effect in $Pb_3(PO_4)_2$. It has been known [7] that a piece of single crystal of $Pb_3(PO_4)_2$ shows extraordinary elastic properties. That is, the single crystal can be deformed like rubber or plastic material under specific shear stress just like the elastic behavior frequently observed in shape-memory (SM) alloys. $Pb_3(PO_4)_2$ undergoes an improper

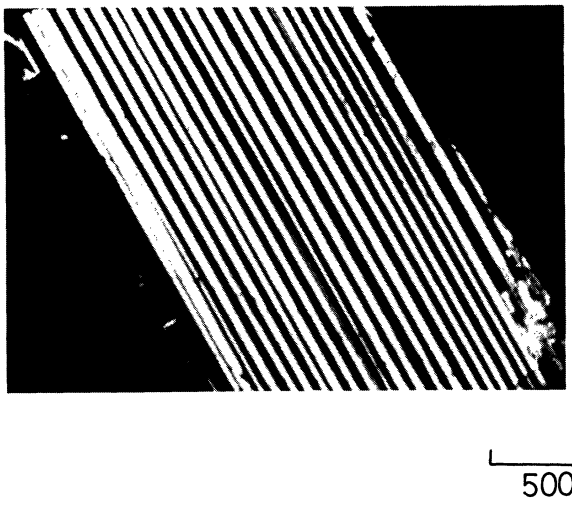

FIG. 1. Typical "stripe"-type domain pattern in a thin plate sample with the face parallel to the $(001)_m$ cleavage plane observed by polarizing optical microscope. The domain boundary is parallel to the mirror plane of the HT rhombohedral phase.

ferroelastic transition at 180 C from rhombohedral $R3m$ (high temperature) phase to monoclinic $C2/c$ (low temperature) phase.[16,17] In the monoclinic phase, there exist three possible ferroelastic variants related to each other by the threefold rotation symmetry of the HT phase.

When single crystals of $Pb_3(PO_4)_2$ are cooled down through the transition temperature, they frequently exhibit a "stripe"-type domain structure, which is characterized by a sequence of alternation of the two (out of the possible three) variants. An example of the stripe domain pattern observed by a polarized microscope is given in Fig. 1.

When pure shear stress was applied on the edge of the specimen parallel to the domain boundaries, they moved to increase the area of the favorable domain to attain the nearly single domain (NSD) state [see Fig. 2(b)]. This procedure resulted in remarkable deformation of the bulk shape. However, it was noticed that even at the highest stressed condition, the perfect single domain state was not obtained, and extremely narrow regions of unfavorable domains were remained always. As the stress was removed, the previous stripe domain structure was recovered [Fig. 1(c)] which resulted in the recovery of the original bulk shape.

The stress-strain relation was measured by the static method. The results are summarized in Fig. 3 by the solid circles. As is seen in the figure, the process is highly nonlinear: the initial response of strain was relatively small, but when the stress exceeded about 20 g/mm^2, the strain increased steeply and finally reached a saturated value which corresponds to the NSD state. The effective elastic constant averaged throughout the whole process was 11.5×10^7 Pa, which was 3 orders of magnitude smaller than the intrinsic elastic constant of $Pb_3(PO_4)_2$, e.g., $c_{11}=4.8\times10^{10}$ Pa, determined by a Brillouin scattering study.[18] Since this effective elastic constant represents the elastic response of the system including many domains, we may call this quantity the pseudoelastic constant.

When the specimen was kept in the NSD state for 72 h under the shear stress at room temperature, the NSD state was maintained even after the removal of the stress. The application of a small stress with the opposite direction transformed the specimen to the previous stripe domain pattern resuming the original shape at the same time, which was found to be also stable. That is, after the aging treatment under the stress, the system has become bistable with respect to the bulk shape. This situation may be interpreted to be the so-called two-way shape memory[1] which is actuated by stress rather than by temperature.

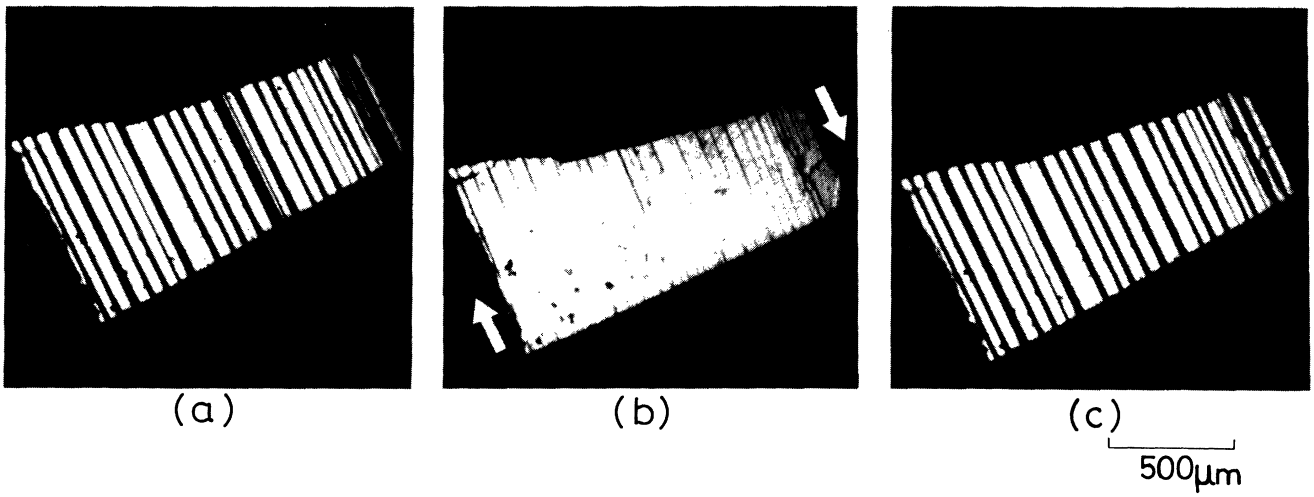

FIG. 2. Reversible change of the stripe pattern during loading-unloading process of the shear stress. (a) Before the stress is applied. (b) A shear stress (indicated by the arrows) is applied. Even at the highest stressed condition, there are extremely narrow regions of unfavorable domain remaining. (c) After the stress is removed.

III. THEORETICAL

A. Landau-scheme

The phase transition mechanism of this material has been well established.[14] The primary order parameters are the amplitudes of the triply degenerated L-point zone boundary phonon modes (η_1,η_2,η_3).[19] There are strong couplings between the order parameters and the macroscopic strains (e_1-e_2,e_6), which belong to a 2D irreducible representation of $3m$ point group. Upon transition, the phonon modes condense to form the static internal distortion of atoms. At the same time, the uniform monoclinic distortion takes place via these couplings, which means that the transition is characterized by an improper ferroelastic transition.

Due to the threefold degeneracy of the primary order parameter, there are three equivalent LT ordered phases:

$$\mathrm{I}^{(')}\text{: } \eta_1=\pm\hat{\eta},\ \eta_2=\eta_3=0,\ e_1-e_2=-\frac{\hat{e}}{2},\ e_6=\frac{\sqrt{3}}{2}\hat{e}\ ,$$

$$\mathrm{II}^{(')}\text{: } \eta_2=\pm\hat{\eta},\ \eta_3=\eta_1=0,\ e_1-e_2=-\frac{\hat{e}}{2},\ e_6=-\frac{\sqrt{3}}{2}\hat{e}\ ,$$

$$\mathrm{III}^{(')}\text{: } \eta_3=\pm\hat{\eta},\ \eta_1=\eta_2=0,\ e_1-e_2=\hat{e},\ e_6=0\ .$$

It should be noticed that in each variant, there are two possible primary order parameter values with opposite signs; $\pm\hat{\eta}$. As pointed out in the previous section, the frequently observed stripe-type domain pattern given in Fig. 1 corresponds to a sequence of alternation of either two of the possible three variants, such as I-II-I′-II′ $\cdots$, the domain boundary coincides with a crystallographic symmetry plane (mirror plane) of the HT phase.[7,20]

B. Ginzburg-Landau scheme

In order to discuss the "thermodynamics of domains," such as the displacement of boundaries under external force, we simply extend the treatment from the Landau scheme to the Ginzburg-Landau scheme. In the GL treatment the order parameter is allowed to be spatially varying; $\xi=\xi(r)$. From this standpoint, a domain boundary is interpreted to be a "kink"-type spatial variation of $\xi(r)$.

The key quantities to be discussed are the equilibrium density of domain boundaries n_k (or equivalently the average domain size, $\bar{l}$), and the response of the order parameter $\langle\xi(X)\rangle_D$ against the external force X conjugate to the order parameter. Here $\langle\cdots\rangle_D$ explicitly indicates that the averaging is to be taken throughout the system containing many kink's. In the present investigation of pseudoelasticity, we are particularly interested in $\langle e(\sigma^{ex})\rangle_D$, where σ^{ex} is the external stress conjugate to the strain e. Formally, this quantity should be expressed by

$$\langle e(\sigma^{ex})\rangle_D=\int\int e(r)P[e(r);\sigma^{ex}]dr\,\delta e(r)\ . \tag{1}$$

Here, $P[e(r)]$ is the probability distribution of $e(r)$ in thermal equilibrium and the second intergration: $\int\cdots\delta e(r)$ means the functional integral in the $e(r)$-functional space.

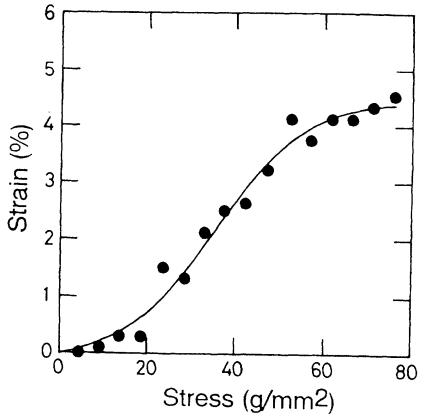

FIG. 3. The stress-strain curve of $Pb_3(PO_4)_2$ with stripe domain measured at room temperature. The solid circles indicate the experimental points. The solid line gives the theoretical curve obtained by Eq. (12) in the text with the parameter values $\bar{\sigma}=35.8$ g/mm^2, $\gamma=16.3$ g/mm^2.

In the following we only discuss the particular case of the stripe-type domain pattern given by the sequence of I-II-I′-II′ $\cdots$. The space variation of the set of the order parameters η_1, η_2, and e_6 corresponding to this stripe pattern would be as shown in Fig. 4(a). The other order parameters η_3 and e_1-e_2 are r independent: $\eta_3=0$, $e_1-e_2=-\hat{e}/2$.

On observing Fig. 4(a), one notices that the domain boundary as shown in Fig. 1 acts as so-called "topological defect" of the pattern, which cannot be annihilated by the application of external stress. As shown in Fig. 4(b), application of stress drives the domain boundaries in the directions to increase the favorable domains. Since the domains with $\eta_1=\pm\hat{\eta}$ are both favorable domains, the antiphase domain boundary associated with η_1 will not be annihilated. This is consistent with the observation that even under highly stressed conditions, there are extremely narrow regions of unfavorable domains remaining [see Fig. 2(b)]. That is, the total number of the boundaries is conserved during the process of applying stress.

The relevant order parameter to discuss the domain formation is expressed by a vector ξ in the 3D subspace of the order parameter space by (η_1,η_2,e_6). The GL free energy is expressed by

$$F=\int_0^L\left[\lambda\left\{\frac{\partial\xi}{\partial X}\right\}^2+f(\xi)\right]dx/d_0\ , \tag{2}$$

where the x direction is taken perpendicular to the stripe domain walls and d_0 is the unit of a microscopic length

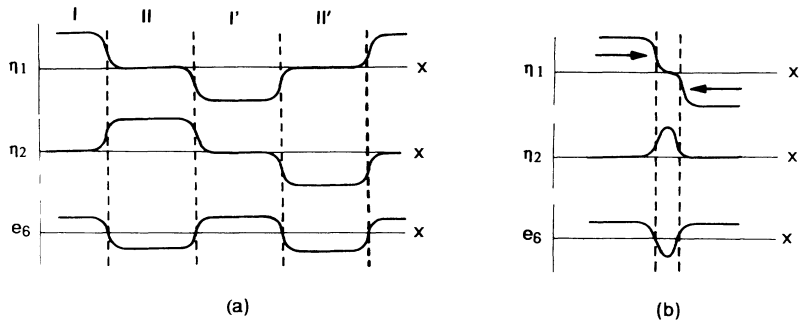

FIG. 4. (a) The spatial variation of the order parameters (η_1,η_2,e_6) along the x axis (the direction perpendicular to the domain boundaries). The kinks correspond to the domain boundaries. The other order parameters (η_3,e_1-e_2) are not x dependent. (b) The spatial variation of $\eta_1(x)$ and $e_6(x)$ under stressed condition. The antiphase boundary between I and I' cannot be annihilated.

scale along the x direction such as the atomic lattice spacing.

One notices that the above expression implies that the system is essentially considered to be a 1D system in the sense that in-plane coupling is so strong that the freedom of the system associated with the spatial variation is allowed only along the x direction. Therefore, we can effectively utilize the transfer-integral (TI) method which is applicable to 1D systems.[21–23] Following the standard procedure of TI method we solve the following eigenvalue equation:

$$\left[\left[\frac{kT\,d_0}{4\lambda}\right]^2\frac{\partial^2}{\partial\xi^2}+f(\xi)\right]\Psi_n(\xi)=\varepsilon_n\Psi_n(\xi)\ . \tag{3}$$

The relevant quantities are then given in terms of eigenvalues and the eigenfunctions by

$$\bar{l}=n_k^{-1}=\frac{kT}{\varepsilon_1-\varepsilon_0}d_0\ , \tag{4}$$

$$\langle\xi_\mu\rangle_D=\int\Psi_0^2(\xi)\xi_\mu d\xi\ , \tag{4'}$$

where ε_0 and ε_1 are the lowest and second lowest energy eigenvalues and Ψ_0 is the eigenfunction for the ground state.[24] In the present case we express the local free energy density $f(\xi)$ in the form

$$f(\xi)=f^0_{(\xi)}+f^R_{(\xi)}\ , \tag{5}$$

$$f^0_{(\xi)}=\frac{\alpha}{2}(\eta_1^2+\eta_2^2)+\frac{\mu_1}{4}(\eta_1^4+\eta_2^4)+\frac{\mu_2}{2}\eta_1^2\eta_2^2 +\frac{1}{4}(c_{11}-c_{12})e_6^2+\lambda_1(\eta_1^2-\eta_2^2)e_6-e^6\sigma^{\rm ex}\ , \tag{6}$$

$$f^R_{(\xi)}=-e_6\sigma^R\ . \tag{6'}$$

The first term $f^0_{(\xi)}$ gives the intrinsic part of the local free energy while the second term $f^R_{(\xi)}$ represents the energy associated with the random stress field which will be inevitably introduced due to imperfection of the crystal.

The intrinsic part f^0 without the last term, is identical to the previously postulated Landau-free-energy density (Ref. 14) except that it is expressed within the 3D subspace spanned by (η_1,η_2,e_6). The last term corresponds to the elastic energy due to the applied shear stress σ_6 corresponding to the experimental procedure as explained in Sec. II.

The eigenvalue equation is formally equivalent to the Schrödinger equation of a fictitious particle moving in the 3D potential given by Eq. (5). The intrinsic potential $f^0_{(\xi)}$ is highly nonlinear having four minima in the 3D order parameter space at $\xi_{\rm I}^{(')}(\pm\hat{\eta},0,\sqrt{3}/2\hat{e})$ and at $\xi_{\rm II}^{(')}(0,\pm\hat{\eta},-\sqrt{3}/2\hat{e})$ (see Fig. 5). Using the equivalence, one can easily infer that the lower eigenstates are analogous to the "tunneling" states of a quantum mechanical particle moving within the four-minimum potential. When the potential barrier between the stable states are sufficiently high as compared to the thermal energy, the lowest four eigenstates are nearly degenerated, and the corresponding eigenfunctions are localized around the local minimum positions $\xi_{\rm I}^{(')}$ and $\xi_{\rm II}^{(')}$. Due to the degeneracy, one sees from Eq. (4) that the average domain size tends to diverge to reach a macroscopic scale. It is practically difficult to estimate the numerical value for $\bar{l}$ (or n_k), since it is sensitive to the parameter λ, for which we have no reliable estimation. At the present stage, let us satisfy ourselves by simply assuming $\bar{l}$ to be order of

$$\bar{l}\sim 10^5 d_0$$

in accordance with the expermental results. In that case the eigenfunction would be completely localized at the minimum of the intrinsic potential. That is,

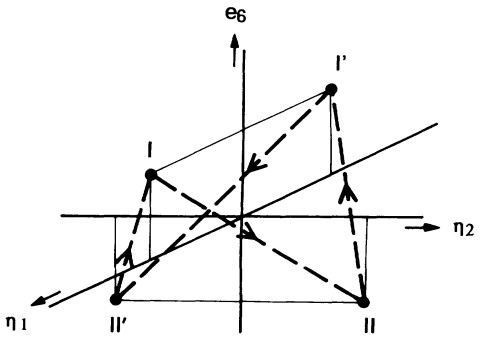

FIG. 5. The tetrastable states of the free energy surface in 3D order parameter space spanned by (η_1,η_2,e_6). The dashed line gives the trajectory followed by the representative point of the system, $\xi(x)$, as the coordinate x is varied.

$$\Psi_0(\xi;\sigma^{\rm ex})=\begin{cases}\delta(\xi-\xi_{\rm I}^{(\prime)}) & \text{when } \sigma^{\rm ex}>0\\ \delta(\xi-\xi_{\rm II}^{(\prime)}) & \text{when } \sigma^{\rm ex}<0\ .\end{cases} \tag{7}$$

While the intrinsic part determines the kink density n_k, the actual spatial configuration of the kinks position $\{x_i\}$, will be determined by the random stress field, so as to minimize the energy:

$$E=\int e_6(x)\sigma^R_{(x)}dx\ , \tag{8}$$

under the condition of fixed n_k. For a kink-type solution of $e_6(x)$, the above energy is expressed by a sum of local pinning potentials:

$$E=\sum_i V_i^P\ . \tag{9}$$

The explicit expression of V_i^P, the pinning potential of the ith kink located at $x=x_i^0$, is given in the Appendix. Thus, the most stable domain configuration is given by the set of $\{x_i^0\}$ giving the minimum value of $\sum_i V_i^P$. It should be noticed that once the random stress field $\sigma^R_{(x)}$ as well as the kink density n_k are given, the stable configuration is uniquely defined, which gives the essential origin of the reversibility of the domain structure before and after the application of external stress, i.e., the origin of the pseudoelasticity.

It is convenient to define the "pinning stress," σ_i^P, of the ith kink by

$$\sigma_i^P=V_i^P/\hat{e}\ . \tag{10}$$

This quantity indicates that under a uniform external stress, $\sigma^{\rm ex}$, the ith kink will be "depinned" when

$$\sigma^{\rm ex}>\sigma_i^P\ .$$

Using σ_i^P we can characterize the given random stress field as follows. For a sufficiently large n_k value, we may assume that the pinning stress in the stable configuration has a distribution in the form of a Gaussian:

$$P(\sigma^P)=e^{-(|\sigma^P|-\bar{\sigma})^2/\gamma^2}/P_0\ , \tag{11}$$

where $\bar{\sigma}$ is the average pinning stress, γ is its variance, and P_0 is the normalization constant. Thus, $\bar{\sigma}$ and γ are considered to be the convenient parameters to specify the characteristics of the random stress field as the pinning centers.

Finally, the bulk strain $\langle e_6\rangle_D$ induced by $\sigma^{\rm ex}$ is given by

$$\langle e_6\rangle_D=\int\int e_6\Psi_0^2(e_6;\sigma^{\rm eff})P(\sigma^P)de_6d\sigma^P\ , \tag{12}$$

$$\sigma^{\rm eff}=\sigma^{\rm ex}-\sigma^P\ , \tag{12'}$$

where $\sigma^{\rm eff}$ represents the effective field to drive the kinks.

Using Eqs. (7), (11), and (12) we calculated $\langle e_6\rangle_D$ versus $\sigma^{\rm ex}$, or the stress-strain curve. The results are given by the solid curve in Fig. 3, where the disposable parameters $\bar{\sigma}$ and γ are adjusted to give the best fit to the experimental results. Notice that, since the number of the kinks (domain boundaries) is conserved in this system, the loading-unloading process should be completely reversible in the present treatment.

Based on the above picture, the (two-way) memory effect is easily understood if we consider that the random stress field σ^R can have time variation with an extremely long relaxation time which will be caused by the diffusion motion of the lattice imperfections such as impurities, vacancies, etc. When the system is kept at the stressed condition for a sufficiently long period (longer than the relaxation time), the built-in random stress field will rearrange itself so as to stabilize the strained configuration of the boundaries. After this process is achieved, the crystal tends to stay on (or "memorize") the deformed state even after the external stress is removed. This is nothing but the observed memory effect.

IV. SUMMARY AND DISCUSSIONS

Summarizing, we have developed a theory of pseudoelasticity in the phenomenological GL scheme. The system with "stripe"-type ferroelastic domain structure has been discussed using the transfer-integral method, which directly gives the equilibrium density of domain boundaries and the response of domain pattern against the external stress. The results are applied to the case of crystal $Pb_3(PO_4)_2$, an ionic material showing pseudoelasticity and shape-memory effect. It is suggested that in this particular case, the random stress field is mainly responsible for pseudoelastic behavior. The observed stress-strain curve has been analyzed quantitatively from this standpoint. The origin of the two-way shape-memory effect has been also inferred from the same standpoint.

In the experimental study, it was observed that even in the highest stressed condition, the domain boundaries are not annihilated. That is, the number of domain boundaries is conserved during the process of applying external stress. In the framework of the present study, the conservation of the number of domain boundaries, n_k, plays the crucial role for the reversibility of the pseudoelastic deformation. The conservation of n_k has been understood as due to the particular symmetry property of the intrinsic free energy which has four stable minima. In this situation, the trajectory of the representative point of the system in the phase space passes through I-II-I′-II′-I $\cdots$ as the coordinate x is varied (see Fig. 5). It should be noted, however, that if the sequence were I-II-I- $\cdots$ instead of I-II-I′ $\cdots$, the pair of kinks is annihilated by the external stress. Since the sums of the individual kink energy are identical for both cases, the realization of the former sequence implies the existence of interactions between neighboring kinks.

In the present treatment, we considered that the domain pattern has been formed as a result of *nonlocal* fluctuations of the order parameter $\xi(r)$. Alternatively, one may propose that ordinary nucleation-growth process has resulted in the domain formation. That is, the nuclei of the LT phase beyond a critical size are *locally* nucleated at random, which continue to grow until they are stopped by collisions with the neighboring domains. The difference of these two mechanism would be manifested in the system size dependence of the resulting domain pattern. In the former case, the average domain

size should be strongly dependent on the system size perpendicular to the domain boundaries, whereas the latter mechanism predicts the pattern to be more or less independent of the system size. It was experimentally observed that in electron micrographs obtained using an extremely thin sample, the same stripe pattern existed, but with an average domain size of order of 100 nm, which is 10^{-2} times smaller than the $\bar{l}$ value shown in Fig. 1. This supports the former viewpoint on which the present treatment is based.

ACKNOWLEDGMENTS

The author would like to thank Professor M. Imada of ISSP, The University of Tokyo and Professor T. Ohta of Ochanomizu University for their valuable discussions.

APPENDIX

We assume that the following condition is satisfied between the three characteristic length scales:

$$\bar{l} \gg \bar{a} \gg \xi_D \ , \tag{A1}$$

where $\bar{a}$ is the average period of the random field $\sigma^R(x)$ and ξ_D is the thickness of a domain wall (see Fig. 6).

The energy gain ΔE due to the displacement Δx of the ith domain wall at $x = x_i$ is given by

$$\Delta E_i \simeq \hat{e}\sigma^R(x_i)\Delta x \ . \tag{A2}$$

Hence, the force, F_i, acting on the domain wall is

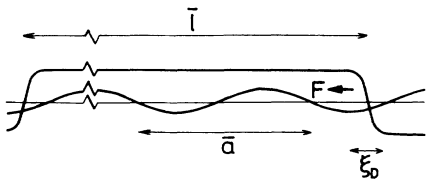

FIG. 6. Postulated geometrical relationship between $\bar{l}$ (average domain size), $\bar{a}$ (average wave length of random stress field), and ξ_D (thickness of the domain boundary). The arrow indicates the force acting on the boundary to displace the kink position.

$$F_i = -\frac{\partial E_i}{\partial x} = -\hat{e}\sigma^R_{(x)} \ . \tag{A3}$$

Therefore, the domain walls should be pinned at the positions $\{x^0\}$ satisfying

$$\sigma^R(x_0) = 0 \ . \tag{A4}$$

By expanding $\sigma^R(x)$ around $x = x^0$, the pinning potential of the boundary at $x = x_i^0$ is estimated to be

$$V_i^P \simeq \hat{e}\xi_D \left[\frac{\partial \sigma^R}{\partial x} \right]_{x = x_i^0} \ . \tag{A5}$$

The most stable domain wall configuration is given by the set of $\{x_i^0\}$ having the minimum value of the total pinning energy $V^P = \sum_i V_i^P$.

[1]K. Otsuka and K. Shimizu, Int. Metals Rev. **31**, 93 (1986).
[2]F. Falk, Acta Metall. **28**, 1773 (1980).
[3]O. Nittono and Y. Koyama, J. Appl. Phys. **21**, 680 (1982).
[4]F. Falk and P. Konopka, J. Phys. Condens. Matter **2**, 61 (1990).
[5]S. Tsunekawa, M. Suezawa, and H. Takei, Phys. Status Solidi A **40**, 437 (1977).
[6]S. Tsunekawa and H. Takei, Phys. Status Solidi A **50**, 695 (1978).
[7]Y. Yamada and Y. Uesu, Solid State Commun. (to be published).
[8]J. M. Kiat, G. Calvarin, and Y. Yamada (unpublished).
[9]M. B. Salamon, M. E. Meichle, and C. M. Wayman, Phys. Rev. B **31**, 7306 (1985).
[10]Y. Yamada, Metall. Trans. **19A**, 777 (1988).
[11]K. Fuchizaki and Y. Yamada, Phys. Rev. B **40**, 4740 (1989).
[12]S. M. Shapiro, Y. Noda, Y. Fujii, and Y. Yamada, Phys. Rev. B **30**, 4314 (1984).
[13]Y. Noda, M. Takimoto, T. Nakagawa, and Y. Yamada, Metall. Trans. **19A**, 265 (1988).
[14]J. Torres, Phys. Status Solidi B **71**, 141 (1975).
[15]C. Joffrin, J. P. Benoit, L. Peschamps, and M. Lambert, J. Phys. (Paris) **38**, 205 (1979).
[16]U. Keppler, Z. Kristallogr. **132**, 228 (1970).
[17]L. H. Brixner, P. E. Bierstedt, W. F. Jaep, and J. R. Barkley, Mat. Res. Bull. **8**, 5128 (1973).
[18]J. P. Chapelle, Cao Xuan An, and J. P. Benoit, Solid State Commun. **19**, 573 (1976).
[19]C. Joffrin, J. B. Benoit, R. Currat, and M. Lambert, J. Phys. (Paris) **40**, 1185 (1979).
[20]U. Bismayer and E. Salje, Acta Crystallogr. A **37**, 1029 (1981).
[21]D. J. Scalapino, M. Sears, and R. A. Ferrell, Phys. Rev. B **6**, 3409 (1972).
[22]D. J. Scalapino, Y. Imary, and P. Pincus, Phys. Rev. B **11**, 2042 (1975).
[23]J. A. Krumhansl and J. R. Schrieffer, Phys. Rev. B **11**, 3535 (1975).
[24]Equation (4) is an approximation valid when the other higher eigenvalues, ε_n's lie far above ε_0: $\varepsilon_n - \varepsilon_0 \gg \varepsilon_1 - \varepsilon_0$, which is just the case of our interest in this paper.

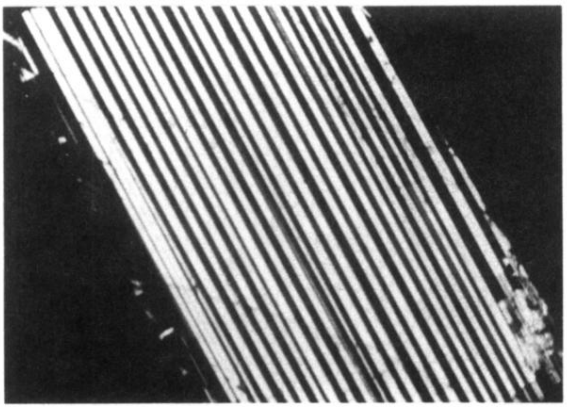

FIG. 1. Typical "stripe"-type domain pattern in a thin plate sample with the face parallel to the $(001)_m$ cleavage plane observed by polarizing optical microscope. The domain boundary is parallel to the mirror plane of the HT rhombohedral phase.

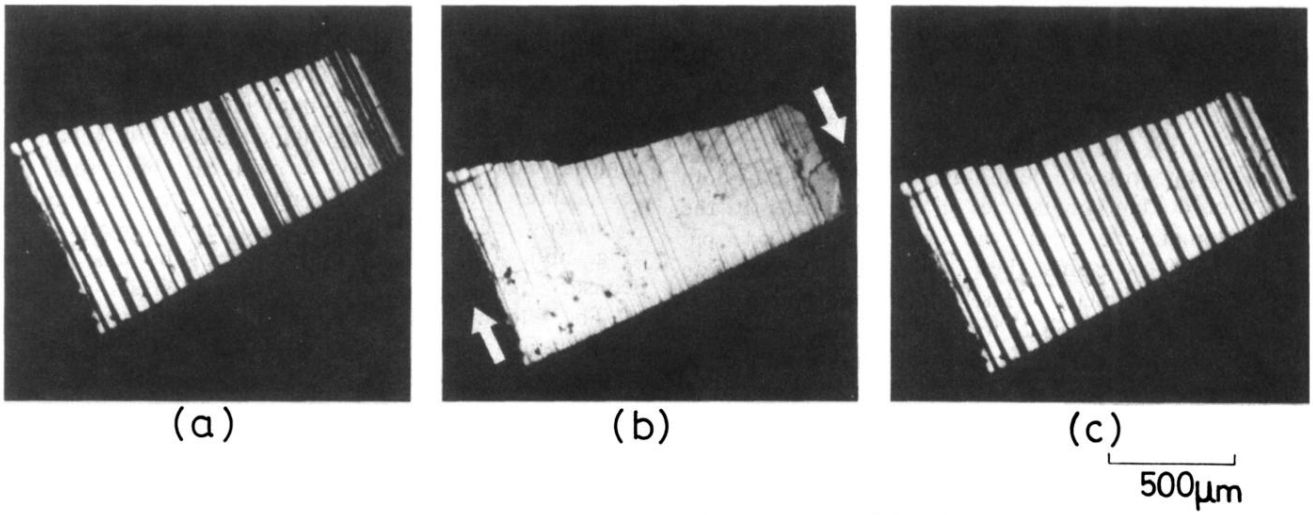

FIG. 2. Reversible change of the stripe pattern during loading-unloading process of the shear stress. (a) Before the stress is applied. (b) A shear stress (indicated by the arrows) is applied. Even at the highest stressed condition, there are extremely narrow regions of unfavorable domain remaining. (c) After the stress is removed.